Chaotic Dynamics of Spin-Valve Oscillators

Z. Yang and S. Zhang
Department of Physics and Astronomy, University of Missouri-Columbia, Columbia, Missouri 65211, USA

Y. Charles Li
Department of Mathematics, University of Missouri-Columbia, Columbia, Missouri 65211, USA
(Received 24 April 2007; published 25 September 2007)

Recent experimental and theoretical studies on the magnetization dynamics driven by an electric current have uncovered a number of unprecedented rich dynamic phenomena. We predict an intrinsic chaotic dynamics that has not been previously anticipated. We explicitly show that the transition to chaotic dynamics occurs through a series of period doubling bifurcations. In chaotic regime, two dramatically different power spectra, one with a well-defined peak and the other with a broadly distributed noise, are identified and explained.

DOI: 10.1103/PhysRevLett.99.134101 PACS numbers: 05.45.Pq, 75.75.+a, 85.75.−d

Among many well-studied nonlinear oscillators driven by external forces, only a handful of oscillators have technological applications [1,2]. The recently discovered current-driven magnetization oscillators with tunable microwave frequencies in spin valves are very desirable for magnetic storage devices and for telecommunications. Up until now, theoretical and experimental studies of the oscillator have been carried out only for the simplest cases where the dynamics of the oscillator is either in a self-sustained steady-state precessional motion (limit cycle) [3–8] or in synchronization with other oscillator(s) [9–13]. Since the equation that governs the oscillator is highly nonlinear, it would be fundamentally interesting to map out the full dynamics for experimentally relevant parameters. In particular, a thorough study of chaotic dynamics will elucidate how the current-driven oscillator responds to an external perturbation.

Previous study of the current-driven magnetization chaos or noise was based on the micromagnetic simulation where the magnetization is not uniform due to strong magnetostatic interaction at the edge of the sample [14,15]. These chaotic dynamics highly depend on the shape and size of the sample, and thus it is not an intrinsic property of the current-driven oscillator. Here we consider a single-domain current-driven spin-valve oscillator so that the undesired complication of the spatial variation of the magnetization is eliminated. The intrinsic dynamic property of the spin-valve oscillator is investigated in the presence of an external periodic perturbation, for example, an ac current. By utilizing the Poincaré map [16], we have found the route to chaos to be via period doubling bifurcations. Positive Lyapunov exponents [16] and Sharkovskii ordering [17] are observed as the evidence of chaos. Furthermore, we show two dramatically different power spectra in chaotic regions, one with a well-defined peak and the other with broadly distributed noise.

The modeled spin valve consists of a pinned layer whose magnetization is fixed along the positive x axis and a single-domain free layer whose magnetization vector $\mathbf{m}$ is the subject of our calculation. The free layer experiences an effective field $\mathbf{H}_{\rm eff}$ made of an external field, an anisotropy, and a demagnetization field perpendicular to the layer (z axis). We choose the direction of the magnetic field along the in-plane easy axis [18]. The dynamics of the magnetization on the free layer is determined by the modified Landau-Lifshitz-Gilbert equation [3]

$$\frac{\partial \mathbf{m}}{\partial t} = -\gamma \mathbf{m} \times \mathbf{H}_{\rm eff} + \alpha \mathbf{m} \times \frac{\partial \mathbf{m}}{\partial t} + a_j \gamma \mathbf{m} \times (\mathbf{m} \times \mathbf{e}_x), \tag{1}$$

where a_j is the amplitude of the spin torque which has the unit of the magnetic field (Oe). Since the magnitude of the magnetization $|\mathbf{m}| = 1$ is a constant, there are only two independent variables, thus, chaotic dynamics are excluded for a constant a_j. In fact, the solutions of Eq. (1) have already been obtained [5,19]. The time-dependent solution is a limit cycle which can be analytically determined via the construction of a Melnikov integral (MI) [5]. It has been found that the stable limit cycle with a well-defined frequency (which we call the natural frequency ω_0) exists only for the current density larger than a critical current density. Two distinct limit cycles have been identified: an out-of-plane orbit and a nearly in-plane orbit around $\mathbf{m} = \mathbf{e}_x$.

To explicitly reveal the dynamics of the above spin-valve oscillator under an external perturbation, we now consider a time-dependent current which adds an additional term in Eq. (1), $a_{ac} \cos(\omega t) \gamma \mathbf{m} \times (\mathbf{m} \times \mathbf{e}_x)$. The simplest dynamic phase would be the synchronization, i.e., the spin-valve oscillator is forced to oscillate in phase with the external frequency ω as long as ω_0 is sufficiently close to ω. Indeed, the recent experiment [9] and theory [12,13] have clearly demonstrated the synchronization. The much richer dynamics, however, would be chaotic dynamics [20] shown below.

An analytical prediction of chaotic dynamics can be made using a MI along the separatrix orbit. The simple zeros of the MI indicate the occurrence of chaotic dynamics [20]. In Ref. [20], the MI was carried out for a fixed magnetic field. Here we map out the phase diagram in a parameter space of both dc current and magnetic field. Implementing the MI approach, we obtain a boundary loop which encloses all the possible simple zeros in the parameter space. In Fig. 1, the phase diagram is plotted. Two solid lines are a portion of the complete boundary loop; if we extend the parameter space to a much larger range, the two lines will meet to form a closed area. Since there exists an arbitrary phase in calculating the MI, the exact solutions are not available. Therefore, a more rigorous numerical test is required to identify the true chaos bounded by the boundary lines. We show below that only the dark region in Fig. 1 is chaos.

Numerically, chaos is often indicated by the positive Lyapunov exponents. The Lyapunov exponent measures the exponential increase (or decrease) of an initial distance from two close trajectories,

$$\lambda_i = \lim_{t\to\infty} \frac{1}{t} \ln \frac{\|\delta m_t^i\|}{\|\delta m_0^i\|}$$

where λ_i is the ith Lyapunov exponent and $\|\delta m_t^i\|$ is the distance between the trajectories of the ith orthogonal axis at time t. When $\lambda_i > 0$, the distance between two arbitrarily close points will increase exponentially along the i axis at a large t [21]. For a bounded dynamic system, any positive Lyapunov exponent indicates chaos. We numerically computed the Lyapunov exponents and Fig. 2(a) shows an example of the Lyapunov spectra, where the largest exponent is shown in red (or gray) solid line and the other two are in dashed and dotted lines. When a_j is smaller than the critical value 230.03 Oe, all three Lyapunov exponents are nonpositive and thus the dynamics are nonchaotic, see Fig. 2(b). When a_j becomes larger than 230.03 Oe, the largest Lyapunov exponents become positive, and thus chaos appears [Fig. 2(c)]. By sweeping the parameters of the dc current and the external field, we have mapped out the parameters that give rise at least one positive Lyapunov exponent, shown as the dark area in Fig. 1.

To understand how chaos develops, we applied the Poincaré map [16,17,21] to this system. In spin-valve oscillators, it is difficult to choose a simple Poincaré section because a simple section can hardly include both out-of-plane and in-plane orbits simultaneously. To avoid this difficulty, we record the trajectory points every time a local minimum of m_x is reached. If we define the time intervals between two successive minima as a period, this is essentially a Poincaré period map except that the period is not a constant.

By using the minimum m_x map, we are able to see the development of chaotic dynamics when one varies the parameters. For limit cycles where the parameters are within the nonchaotic white regions shown in Fig. 1, the magnetization follows a unique trajectory and the map point is just one unique point. When the parameters, e.g., the currents, are close to the boundaries between the white and dark regions of Fig. 1, two map points are seen; this is identified as the period doubling bifurcation. In this case, the magnetization orbit will return to the original orbit after two periods. If we choose the current even closer to the boundaries, a period-four orbit and, in general, a period-2^n orbit, appear. When $n \to \infty$, the magnetization dynamics

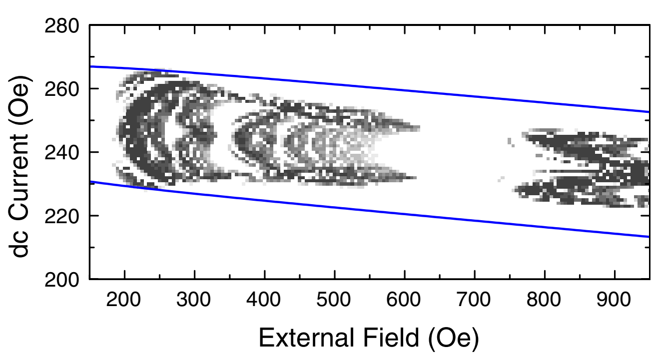

FIG. 1 (color online). Chaotic-nonchaotic phase diagram. Two lines are the boundary of chaos determined by the Melnikov integral. Chaos is possible only within the region bounded by these two lines. The dark region represents a positive value of the largest Lyapunov exponent, i.e., chaos. The parameters are chosen similar to a permalloy film: damping constant $\alpha = 0.02$, anisotropy constant $H_K = 0$, demagnetization field $4\pi M_s = 8400$ Oe, and $\gamma = 1.7 \times 10^{-7}$ Oe^{-1} s^{-1}. The amplitude and the frequency of the ac current are $a_{ac} = 20$ Oe and $\omega = 15$ GHz.

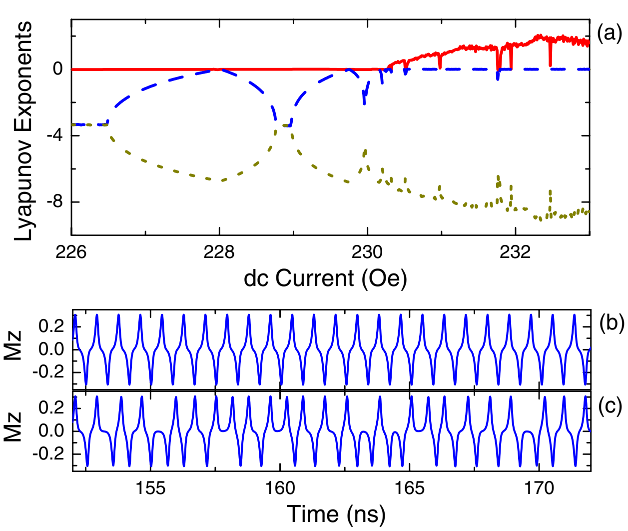

FIG. 2 (color online). (a) Lyapunov spectra for 226 Oe $< a_j <$ 233 Oe; (b) the regular nonchaotic trajectory for $a_j = 227.5$ Oe; (c) chaotic trajectory for $a_j = 232.5$ Oe. The magnetic field is 200 Oe. All parameters are the same as in Fig. 1.

become chaotic, i.e., the appearance of the dark regions in Fig. 1. In Fig. 3, we have shown an example of the bifurcation diagram where the transition from the synchronization to the bifurcation and to chaos is clearly demonstrated. Period-five and period-six chaos windows are observed between 252 to 253 Oe in the cascade. According to Sharkovskii ordering theorem, these observations imply the existence of chaos [17].

The period doubling bifurcation cascade shown in Fig. 3 is in fact similar to those in other nonlinear systems [16]. To see if our bifurcation structure belongs to the same universal quadratic class, we evaluate the Feigenbaum ratio [22] which is defined as

$$\delta_i = \frac{a_i - a_{i+1}}{a_{i+1} - a_{i+2}},$$

where a_i is the value of the parameter at the ith bifurcation point. In Table I, We list an example of measurement of Feigenbaum ratios for our system. There is a second Feigenbaum ratio that denotes the rescaling ratio of the bifurcation forks. For example, from first two bifurcation in Fig. 3, we measured $|\alpha| = |\Delta M_{x1}/\Delta M_{x2}| = 2.68$. Analytically, the Feigenbaum ratios are approaching to the universal constants 4.6692... for δ and 2.5029... for $|\alpha|$ [22], for a quadratic nonlinear map [23]. We find that the measured ratios agree with the universal Feigenbaum numbers exceedingly well. This indicates that our system indeed belongs to a quadratic nonlinear class.

By summing all Lyapunov components, we have verified that the volume contraction ($\lambda_v = \lambda_1 + \lambda_2 + \lambda_3$) is always negative even though the Lyapunov exponent can be positive; the negative volume contraction indicates the dissipative nature of the spin-valve oscillator [16,21].

A highly interesting feature is the two distinct magnetization trajectories during the transition to chaos. In the first case, the bifurcation occurs only at the out-of-plane orbits shown in Fig. 4(a). Although the bifurcation on this single orbit also leads to chaos because the largest calculated Lyapunov exponent is positive, the power spectrum displays a well-defined peak. The peak position corresponds to the inverse of the average time for the magnetization to complete one loop (since the loop never closes, we define a one-loop when the trajectory returns to the point nearest to the starting point of the loop). Thus, the presence of the narrow peak indicates a quasiperiodic motion of the magnetization in chaotic dynamics. It would be erroneous if one automatically assumes the dynamics is synchronization when the experimental power spectrum is highly peaked. Synchronization refers to the phase locking between the external and natural frequencies, but the positive Lyapunov exponent excludes the possibility of the phase locking. The second chaotic motion involves both out-of-plane and in-plane orbits, as seen in Fig. 4(c). In this case, the power spectra display typical noise, i.e., broadly distributed spectra. The magnetization jumps between out-of-plane and in-plane orbits are completely random; it is an intrinsic stochastic process driven by a deterministic external perturbation. This stochastic jumping leads to a much stronger noise in the power spectra. On the other hand, it is necessary that trajectories are within the vicinity of the separatrix of two different orbits so that the stochastic magnetization jump can take place under small perturbations. Since the separatrix has an infinite period, the trajectory close to it must have a nearly zero frequency as seen in Fig. 4(d).

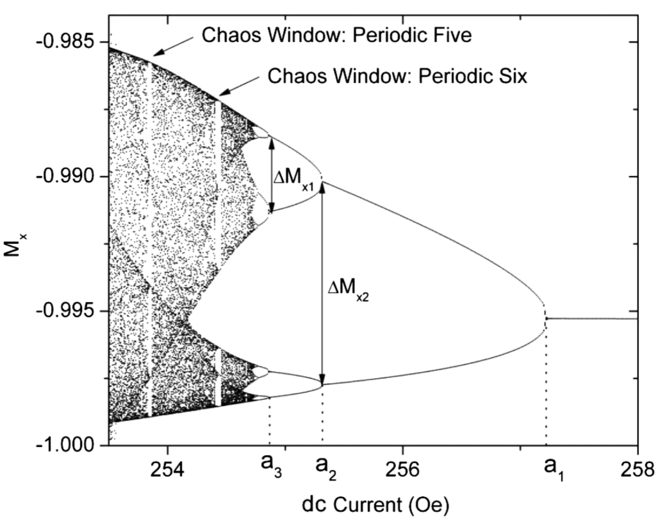

FIG. 3. Period doubling bifurcation cascade. The dashed lines indicate the critical values of the dc current where the bifurcation occurs. All parameters are the same as in Fig. 2.

The synchronizationlike chaotic power spectra imply that quasiperiodicity can be observed in chaos if the trajectory is not near the separatrix. It is the stochastic jump of the trajectory in the vicinity of the separatrix that reduces the periodicity. The reduction of the periodicity due to stochastic jumps could also occur when the thermal fluctuations exist because the thermal fluctuations are stochastic, known as a Wiener process. In general, there exists a bifurcation gap [24] where the thermal fluctuations limit the observation of 2^n orbits in the bifurcation diagram to a finite number $n < n_0$. The stronger the fluctuations are, the smaller n_0 is. Consequently, the thermal fluctuations make

TABLE I. Feigenbaum ratio measurement. The second column is derived from Fig. 3; a_i is a critical value at the ith bifurcation point.

i	a_i	$a_i - a_{i+1}$	δ_i
1	257.2500	−1.9300	4.289
2	255.3200	−0.4500	4.356
3	254.8700	−0.1033	4.472
4	254.7667	−0.0231	4.529
5	254.7436	−0.0051	4.636
6	254.7385	−0.0011	
7	254.7374		

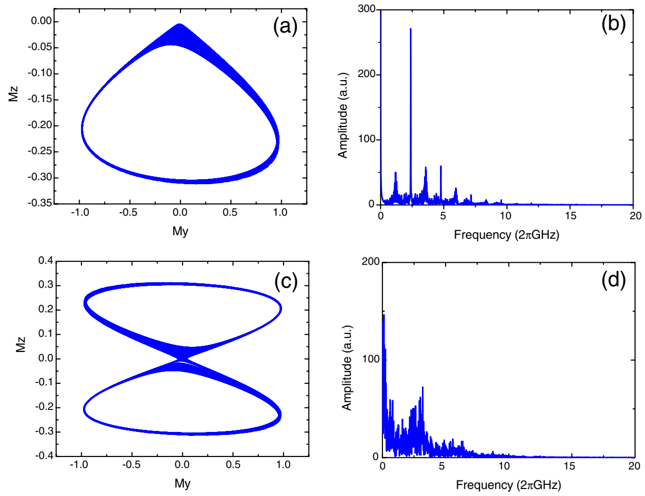

FIG. 4 (color online). Trajectories and their corresponding M_z-component power spectra of two types of chaos. Upper panels: $a_j = 262.5$ Oe; the largest Lyapunov exponent is 0.86. Lower panels: $a_j = 261.0$ Oe; the largest Lyapunov exponent is 1.56. All parameters are the same as in Fig. 2.

the Lyapunov spectra smoother in Fig. 2 and chaos windows invisible in Fig. 3. We emphasize that although the thermal fluctuations lead to noise in the power spectra and the possible random jumps between two orbits, it is not associated with the bifurcation and thus there are no universal Feigenbaum numbers. Experimentally, one can distinguish chaotic dynamics generated by the deterministic perturbation (ac current) and by the thermal fluctuations. For example, when the parameter, e.g., dc current in our study, is varied, the current-driven power spectrum should evolve from nonchaotic dynamics to chaos and back to nonchaos.

In conclusion, by using both analytical and numerical approaches, we have shown the route to chaos and that the oscillator belongs to the class of dissipative quadratic nonlinear systems. Our findings demonstrate that the current-driven magnetization dynamics is much richer than previously studied steady-state motion and synchronization. The magnetization oscillator whose dynamics can be measured by experiments provides a model system to verify chaos theories in a general nonlinear system.

This work was supported by DOE(DE-FG02-06ER46307).

[1] A. Pikovsky, M. Rosenblum, and J. Kurths, *Synchronization: A Universal Concept in Nonlinear Sciences* (Cambridge University Press, Cambridge, U.K., 2001).
[2] M. I. Rabinovich and D. I. Trubetskov, *Oscillations and Waves in Linear and Nonlinear Systems* (Kluwer, Dordrecht, 1989).
[3] J. C. Slonczewski, J. Magn. Magn. Mater. **159**, L1 (1996); **195**, 261 (1999).
[4] J. Z. Sun, Phys. Rev. B **62**, 570 (2000).
[5] G. Bertotti, C. Serpico, I. D. Mayergoyz, A. Magni, M. d'Aquino, and R. Bonin, Phys. Rev. Lett. **94**, 127206 (2005).
[6] S. I. Kiselev, J. C. Sankey, I. N. Krivorotov, N. C. Emley, R. J. Schoelkopf, R. A. Buhrman, and D. C. Ralph, Nature (London) **425**, 380 (2003).
[7] I. N. Krivorotov, N. C. Emley, J. C. Sankey, S. I. Kiselev, D. C. Ralph, and R. A. Buhrman, Science **307**, 228 (2005).
[8] Z. Li and S. Zhang, Phys. Rev. B **68**, 024404 (2003).
[9] W. H. Rippard, M. R. Pufall, S. Kaka, T. J. Silva, S. E. Russek, and J. A. Katine, Phys. Rev. Lett. **95**, 067203 (2005).
[10] S. Kaka, M. R. Pufall, W. H. Rippard, T. J. Silva, S. E. Russek, and J. A. Katine, Nature (London) **437**, 389 (2005).
[11] F. B. Mancoff, N. D. Rizzo, B. N. Engel, and S. Tehrani, Nature (London) **437**, 393 (2005).
[12] J. Grollier, V. Cros, and A. Fert, Phys. Rev. B **73**, 060409(R) (2006).
[13] A. N. Slavin and V. S. Tiberkevich, Phys. Rev. B **72**, 092407 (2005).
[14] K. -J. Lee, A. Deac, O. Redon, J. -P. Nozières, and B. Dieny, Nat. Mater. **3**, 877 (2004).
[15] D. V. Berkov and N. L. Gorn, Phys. Rev. B **71**, 052403 (2005); **72**, 094401 (2005).
[16] K. T. Alligood, T. D. Sauer, and J. A. Yorke, *Chaos: An Introduction to Dynamical Systems* (Springer, New York, 1997).
[17] E. Ott, *Chaos in Dynamical Systems* (Cambridge University Press, New York, 2002).
[18] Experimentally, the observation of the precessional states and synchronization was made for the magnetic field at an angle to the film plane. The primary reason is that the limit cycle or the precessional state generally occurs at a much wider range of parameters for the field applied at an angle to the plane than for the field in the plane. Thus it is easier for experiments to observe the limit cycle in the former case. For our theoretical study of chaotic dynamics, it is natural to minimize the additional parameter (the direction of the field) by choosing the field along the easy axis. We expect that there is no fundamental difference with respect to the direction of the field.
[19] C. Serpico, M. d'Aquino, G. Bertotti, and I. D. Mayergoyz, J. Magn. Magn. Mater. **290–291**, 502 (2005).
[20] Z. Li, Y. C. Li, and S. Zhang, Phys. Rev. B **74**, 054417 (2006).
[21] J. M. González-Miranda, *Synchronization and Control of Chaos: An Introduction for Scientists and Engineers* (Imperial College Press, London, 2004).
[22] M. J. Feigenbaum, J. Stat. Phys. **19**, 25 (1978).
[23] J. P. Van Der Weele, H. W. Capel, and R. Kluiving, Physica (Amsterdam) **145A**, 425 (1987).
[24] J. P. Crutchfield, J. D. Farmer, and B. A. Huberman, Phys. Rep. **92**, 45 (1982).